2012

MscS-Like10 is a stretch-activated ion channel from Arabidopsis thaliana with a preference for anions

Grigory Maksaev
Washington University in St Louis

Elizabeth S. Haswell
Washington University in St Louis, ehaswell@wustl.edu

Biological Sciences

Plant Biology

MscS-Like10 is a stretch-activated ion channel from *Arabidopsis thaliana* with a preference for anions

Grigory Maksaev and Elizabeth S. Haswell*

Department of Biology, Campus Box 1137
One Brookings Drive
Washington University in Saint Louis
Saint Louis, MO 63130

*Corresponding Author
Tel: (314) 935-9223
Email: ehaswell@wustl.edu

ABSTRACT

Like many other organisms, plants are capable of sensing and responding to mechanical stimuli such as touch, osmotic pressure and gravity. One mechanism for the perception of force is the activation of mechanosensitive (or stretch-activated) ion channels, and a number of mechanosensitive channel activities have been described in plant membranes. Based on their homology to the bacterial mechanosensitive channel MscS, the ten MscS-Like (MSL) proteins of *Arabidopsis thaliana* have been hypothesized to form mechanosensitive channels in plant cell and organelle membranes. However, definitive proof that MSLs form mechanosensitive channels has been lacking. Here we used single-channel patch clamp electrophysiology to show that MSL10 is capable of providing a MS channel activity when heterologously expressed in *Xenopus laevis* oocytes. This channel had a conductance of ~100 pS, consistent with the hypothesis that it underlies an activity previously observed in the plasma membrane of plant root cells (Haswell ES et al. (2008) Curr Biol 18:730-4). We found that MSL10 formed a channel with a moderate preference for anions, which was modulated by strongly positive and negative membrane potentials, and was reversibly inhibited by gadolinium, a known inhibitor of mechanosensitive channels. MSL10 demonstrated asymmetric activation/inactivation kinetics, with the channel closing at substantially lower tensions than channel opening. The electrophysiological characterization of MSL10 reported here provides insight into the evolution of structure and function of this important family of proteins.

37 **/body INTRODUCTION**

38 The perception of mechanical stimuli like gravity, touch or osmotic pressure is essential to
39 normal plant growth and development, and is further implicated in biotic and abiotic stress
40 responses (1). One of the best-studied strategies for perceiving force involves membrane-
41 embedded channels that are gated by tension, known as mechanosensitive (MS) channels (2).
42 Numerous MS channel activities (> 17 to date) have been described in the membranes of
43 diverse tissues from a wide variety of plant species (summarized in (3), also (4, 5)). Many of
44 these observed MS channel activities differ in their conductance, ion selectivity, and/or
45 sensitivity to the direction of activation pressure, suggesting that multiple classes of
46 mechanosensitive channels are present in plant cells.

47

48 No mechanosensitive ion channel activity discovered in plant membranes has yet been
49 definitively identified at the molecular level, but two families of proteins serve as strong
50 candidates. The first is the Mid1-Complementing Activity (MCA) family, members of which are
51 required for root response to touch in the model plant *Arabidopsis thaliana*, induce Ca^{2+} uptake
52 in rice and Arabidopsis cells (6, 7), and are associated with increased current in response to
53 hypotonic stimulation of Xenopus oocytes (8). The second family of candidates for plant MS
54 channels is the MscS-Like (MSL) family, first identified based on modest homology to the well-
55 characterized bacterial MS channel MscS from *Escherichia coli* (3, 9). MscS is a largely non-
56 selective stretch-activated channel that is gated directly by membrane tension, generating a 1
57 nanoSiemen (nS) conductance (reviewed in (10, 11)). The primary function of MscS is to provide
58 a conduit for the release of osmolytes from the bacterium in response to extreme hypoosmotic
59 stress (12, 13).

60

61 There are ten MscS homologs in Arabidopsis, three with predicted or observed localization to
62 organellar membranes and seven with predicted or observed localization to the plasma and
63 vacuolar membranes (3, 5, 14). Reverse genetic analyses have demonstrated that two plastid-
64 localized homologs, MSL2 and MSL3, are required for the proper size, shape, division, and
65 hypoosmotic volume control of plastids (14-16). In addition, two plasma membrane-localized
66 homologs, MSL9 and MSL10, are genetically required for the predominant MS channel activity
67 in the plasma membrane of Arabidopsis root cell protoplasts, providing support for the
68 hypothesis that MSL proteins form MS channels (5). A MscS homolog from the unicellular green
69 alga *Chlamydomonas reinhardtii,* MSC1*,* has MS channel activity when expressed in giant *E. coli*
70 spheroplasts (17).
71
72 However, it has been proposed that the contribution of MSL9 and MSL10 to MS channel activity
73 in root protoplasts may be indirect (1), and a more rigorous test by expression and
74 electrophysiological characterization in a heterologous system is needed. Indeed it seems likely
75 that MSLs do not form MS channels, as the plasma membrane-localized MscS homologs from
76 plants are highly divergent from MscS with respect to topology and show limited sequence
77 similarity, even within the conserved domain (Fig. S*1*). Some bacterial MscS homologs do not
78 appear to provide MS channel activities, further suggesting that a subset of the family has
79 evolved to perform diverse functions (reviewed in (18)). We were thus motivated to develop a
80 system for the electrophysiological investigation of MSL proteins to determine if eukaryotic
81 plasma membrane-localized MscS homologs indeed form MS channels, and if so, to compare
82 their electrophysiological behavior with that of other MscS homologs. Here we describe the
83 heterologous expression and characterization of Arabidopsis MSL10 in *Xenopus laevis* oocytes.

84 **RESULTS**

85

86 ***MSL10 forms a ~100 pS mechanosensitive channel in the plasma membrane of Xenopus***
87 ***oocytes.*** We chose to characterize MSL10 in *Xenopus laevis* oocytes, an established system for
88 the expression and electrophysiological characterization of heterologous ion channels,
89 including those from plants (19). The endogenous MS channels of Xenopus (20) were effectively
90 inactivated upon excision of the membrane patch, as previously reported (21). Xenopus oocytes
91 produced strong GFP signal at their periphery by 48 hours after injection with MSL10-GFP
92 cRNA, indicating that the MSL10 protein is efficiently translated and localized to the plasma
93 membrane (Fig. 1*A*).

94

95 Inside-out patches excised from oocytes injected with cRNA encoding either MSL10-GFP or
96 untagged MSL10 reproducibly exhibited channel activity in response to membrane stretch in
97 symmetric ND96 buffer (Fig. 1*B*), though we consistently observed more activity when
98 untagged MSL10 was used. MSL10 channel activity was dependent on an increase in membrane
99 tension, but we reproducibly observed that the same tension resulted in different current
100 amplitudes at opposite membrane potentials in the same patch (representative traces are
101 shown in Figure 1*B*). Under negative membrane potentials, MSL10 single-channel events were
102 easy to observe due to low noise and their stable behavior, while under positive membrane
103 potentials noise and flickery behavior were dominant. The ratio of peak current amplitude at
104 negative to positive membrane potentials was 1.24 ± 0.15 (n = 7 oocytes). The results at
105 negative membrane potentials are most likely to represent the behavior of the MSL10 *in planta*,
106 as the transmembrane potential of Arabidopsis root cells has been measured at about -180 mV

107 (for example, see (22)). MSL10 single-channel openings were readily detected in response to
108 membrane stretch generated by both negative (Fig. 1*C*) and positive (Fig. 1*D*) pipette pressures.
109
110 The current-voltage (I/V) curves for MSL10 and MSL10-GFP indicated that the single channel
111 conductances of both MSL10 and MSL10-GFP were 103 ± 3 pS in excised patches, measured as
112 the slope of the I/V curve within the range of 0 to -60 mV (Fig. 2*A*). We did not use data from
113 potentials lower than -60 mV in our calculation of conductance due to the presence of
114 conducting substates (an example of which is shown in Figure 2*B*). A conductance of 103 ± 3 pS
115 is in good agreement with an MSL10-dependent activity present in Arabidopsis root
116 protoplasts, which was measured at 137 pS under slightly different ionic conditions (5). Though
117 the I/V curve for MSL10 was linear at positive and negative membrane potentials, the slopes
118 were slightly different under the two conditions, with a single-channel conductance of 80 ± 2 pS
119 at positive membrane potentials (0 to +60 mV), or 1.3-fold lower than at negative potentials.
120 This slight current rectification may explain the 1.24-fold difference in current under positive
121 and negative potentials described above and shown in Figure 1*B*.
122
123 ***MSL10 exhibits a moderate preference for anions***. The reversal potential of MSL10 under
124 asymmetric 100/300 mM salt was -19 mV (Fig. 3*A*), while the theoretical reversal potential of Cl^-
125 ion, derived from the Nernst equation under a three-fold gradient of ion concentration, is -28
126 mV. The Goldman-Hodgkin-Katz equation gives a ratio of Cl^- to Na^+ permeability ($P_{Cl} : P_{Na}$) of 5.9
127 for MSL10. We also measured the conductance of MSL10 when Na^+ was replaced with TEA^+, a
128 large ion with an estimated diameter of ~ 8 Å (23)) often used as a pore blocker of potassium
129 channels (24, 25). As Hille's equation (26) also predicts an approximate pore diameter of 8 Å for
130 MSL10 (assuming a uniform cylinder 5 nm in length) TEA^+ is not likely to permeate the MSL10

131 channel pore; nor does TEA^+ serve to block MSL10 (Fig. 2*A*). The single-channel conductance of
132 MSL10 in 100 mM symmetric TEA-Cl was ~84% of that measured in symmetric ND96 (96 mM
133 NaCl). This result is consistent with the $P_{Cl} : P_{Na}$ ratio of 5.9 for MSL10 calculated from Figure 3*A*,
134 which predicts that 83% of the MSL10 current in ND96 is provided by Cl^-. The MSL10-dependent
135 ion channel activity previously characterized in root protoplasts showed no change in
136 conductance when $CaCl_2$ in the bath solution was replaced with TEA-Cl, while current was
137 abolished when Cl^- was replaced with MES^-—indicating that neither Ca^{2+} nor TEA^+ can permeate
138 the channel (5). MSL10 single-channel conductance showed saturation at relatively low ionic
139 strength at both positive and negative membrane potentials (Fig. 3*B*). In summary, MSL10
140 forms a channel with a moderate preference for anions, passing approximately 6 chloride ions
141 for every sodium ion.
142
143 ***MSL10 is reversibly inhibited by Gd^{3+} ions in inside-out patches***. Gadolinium ions are commonly
144 used to inhibit K^+-, Ca^{2+}- and metazoan MS channels (27), and have also been demonstrated to
145 inhibit the activity of MS channels in plants (28-30) and bacteria (31). Inhibition of MSL10
146 activity was observed after excised inside-out patches were perfused in a bath containing 100
147 µM $GdCl_3$ (Fig. 3*D*). This inhibition was reversible, as MSL10 activity was recovered upon Gd^{3+}
148 washout. Less effective inhibition was observed in patches perfused with 50 or 20 µM $GdCl_3$
149 (Fig. 3*E* and *F*), and an identical regime on outside-out patches did not significantly inhibit
150 MSL10 activity (Fig. 3*C*).
151
152 ***MSL10 gating kinetics and inactivation.*** As shown in Fig. 1*B-D*, all MSL10 traces—regardless of
153 pipette size, transmembrane potential or amount of applied pressure—exhibited a peak
154 tension-induced current that was delayed compared to the peak of applied pressure. We used

155 relatively fast ramp speeds (~1 sec) in our initial characterization of MSL10, in accordance with
156 previous studies of MscS (e.g. (32)) and to reduce artifacts associated with changes in patch
157 structure during recordings (33). Substantially slower ramp speeds (~25 sec) still produced the
158 observed asymmetric pressure-dependence of channel opening and closing, and did not
159 depend on the number of activated channels (Fig. 4*A*, *B*). Increasing the Mg^{2+} concentration of
160 bath and pipette solutions, which has been shown to improve membrane-glass adhesion and
161 facilitate gigaseal formation (34), did not alter the slow closing behavior of MSL10 (Fig. S2*A*, *B*).
162 Finally, we sequentially applied pressure ramps of different lengths (1s, 5s and 25s) to the same
163 patch and compared the pressure at which the first channels opened or the last channels closed
164 at each ramp speed (Fig. S3). The threshold pressure required to open MSL10 channels was
165 reduced with slower ramp speeds, dropping 1.42 ± 0.17-fold between 1s and 5s ramps and 2.19
166 ± 0.34-fold between 1s and 25s ramps (n = 7 patches). In contrast, the ramp pressure at which
167 all MSL10 channels had closed was always below the opening threshold pressure, regardless of
168 the pressure ramp speed. In more than half of these experiments, the last MSL10 channel
169 closed under zero applied pressure. We were not able to utilize the midpoint gating tension in
170 our characterization of MSL10, as the oocyte membrane routinely ruptured before current
171 saturation regardless of pressure ramp length, though this was not observed with MscS under
172 the same conditions (Figure S4*A*, *B*).
173
174 To gain further insight into MSL10 gating kinetics and adaptive behavior, we applied tension to
175 the membrane in multiple sharp steps, as previously reported for MscS (35). Under these
176 conditions, MSL10 displayed very slow opening and closing kinetics compared to MscS, even
177 after multiple cycles (Fig. 4*C*). Occasionally a fraction of the channels stayed in the open state
178 and did not close after pressure release at higher potentials (Fig. S2*B*). These data indicate that,

179 under a variety of experimental conditions, the MSL10 channel closes at a much lower tension
180 than is required for it to open, and in some conditions can remain open even in the absence of
181 applied pressure. Unlike MscS, which enters a tension-unresponsive state after sustained
182 stimulus (12, 32), we did not detect inactivation of MSL10 even after 10-20 seconds of
183 sustained tension (Fig. 4*C* and S2*B*).

184 **DISCUSSION**

185

186 The presence of multiple diverse mechanosensitive (MS) ion channel activities in the plasma
187 and vacuolar membranes of land plants has been well documented over the past 20 years
188 (summarized in (3)), and two candidate gene families have been identified in the model plant
189 *Arabidopsis thaliana* (reviewed in (1)). Here we used single-channel patch clamp
190 electrophysiology to provide direct evidence that a member of one of these families, MSL10,
191 provides a stretch-activated channel activity when heterologously expressed *in Xenopus laevis*
192 oocytes. MSL10 is likely to represent the activity previously described in the root protoplasts of
193 a *msl9-1; msl10-1* double mutant transiently expressing MSL10, an anion-preferring channel
194 with a conductance of ~137 pS at -182 mV (5). Though we were unable to measure MSL10
195 channel conductance in oocytes at such high potentials, this value is close to the conductance
196 of oocyte-expressed MSL10 under our conditions (103 pS at 0 to -60 mV). In addition to the
197 activity in roots that we can now assign to MSL10, a non-selective channel activity described in
198 Arabidopsis leaf mesophyll cells (36) also shows a preference for anions (P_{Cl} : P_K ratio of 1.9),
199 and may represent the activity of MSL10 or another MscS homolog.

200

201 Our characterization of MSL10 channel behavior provides insight into the evolutionary
202 conservation of structure and function between MscS homologs. Figure S1 shows the known or
203 predicted topology of MscS, MSL10, MSC1, and YbdG, a MscS homolog from *Escherichia coli* to
204 which we refer here as MscM (37, 38). MSL10 has an extended N-terminus and a total of 6 TM
205 helices, while MSC1 and MscM have 5 and MscS has 3 TM helices. The conserved "MscS
206 domain" as defined here comprises the most C-terminal TM helix (TM3 in MscS) and the upper
207 portion of the hollow cytoplasmic domain, called the β-domain (Fig. S1*A*, *B* (39)).

208

209 Numerous studies on MscS have indicated the functional importance of the residues within the
210 conserved region, primarily in the pore-lining TM3 helix (summarized in (40)). For example, the
211 characteristic alteration between small and large hydrophobic residues appear to be
212 responsible for proper TM3 packing in the MscS heptamer (41) and the hydrophobic seal
213 residues L105 and L109 are essential for complete channel closure (39, 41-44). While these
214 structural motifs are for the most part preserved in MscM and MSC1, MSL10 shares very little
215 homology in the predicted pore-lining region (Fig. S1*C*), instead exhibiting many bulky
216 hydrophobic residues—including six phenylalanines—in the TM3 region. It is therefore
217 surprising that MSL10 has MS channel activity at all, and perhaps even more surprising how
218 closely MSL10 behavior resembles MscS, MscM, and/or MSC1.

219

220 ***1) Unitary conductance.*** MSL10 had a unitary conductance of 103 ± 3 pS in symmetric 100 mM
221 NaCl, while MscS has a conductance of 330 pS under the same conditions (21) (about 1 nS when
222 measured in 200 mM KCl, 90 mM $MgCl_2$ and 10 mM $CaCl_2$ (32, 41, 45)). Though MscM and
223 MSC1 are highly similar to MscS with respect to the sequence of the pore-lining TM3 helix, they
224 have conductances similar to that of MSL10: 100-150 pS in 100 mM KCl for MscM (37, 38) and
225 400 pS for MSC1 measured in 200 mM KCl with 40 mM $MgCl_2$ and 10 mM $CaCl_2$ (17) (120-130
226 pS if measured in 100 mM salt). While it is tempting to speculate that the many bulky
227 hydrophobic residues in the pore-lining helix of MSL10 may be responsible for a smaller pore
228 size—and therefore a smaller conductance than MscS—the smaller conductances of MscM and
229 MSC1 require a different explanation.

230

231 **2*) Ion selectivity.*** Though formally non-selective, the MSL10 channel showed a preference for
232 anions, with a $P_{Cl} : P_{Na}$ ratio of 5.9 based on reversal potential and on its conductance when Na^+
233 was replaced with TEA^+ (Figs. 2*A*, 3*A*). Other MscS family members display diverse ion
234 selectivity; MscS demonstrates a weak preference for anions with $P_{Cl} : P_K$ = 1.2 – 3.0 (45-48),
235 MscM a weak preference for cations, with $P_{Cl} : P_K$ = 0.4 (37) and MSC1 is as anion-selective as
236 MSL10, with $P_{Cl} : P_K$ = 7 (17). MSL10 also showed saturation with increased solution conductivity
237 at both positive and negative membrane potentials (Fig. 3*B*). A conductance ratio of about 1.3
238 (negative membrane potential to positive membrane potential) was observed in these
239 experiments, similar to that measured in symmetric ND96 (Fig. 2*B*). While MscS does not show
240 saturation up to 1.5M KCl (46), a MscS homolog from the soil bacterium *Corynebacterium*
241 *glutamicum* saturated at negative but not at positive membrane voltages (49).
242
243 Gadolinium is a potent inhibitor of mechanosensitive channels of various types (27, 30, 50, 51),
244 but different mechanisms are likely to be involved in each case. Gd^{3+} ions inhibit Ca^{2+}-selective
245 stretch-activated channels at concentrations as low as 1 µM (30), but concentrations above 100
246 µM are required to inhibit the essentially non-selective bacterial channels MscS and MscL (31,
247 51). In the later case, gadolinium ions have been shown to inhibit MS channels through
248 interactions with negatively charged lipids in the membrane (51). Efficient inhibition of MSL10
249 in inside-out patches was produced only at the highest concentration of gadolinium tested, 100
250 µM (Fig. 3*D*, *E*, *F)*. Even in this case, increased tension evoked partial restoration of channel
251 activity. As the inside but not the outside of the oocyte membranes contain the negatively
252 charged lipids proposed to interact with Gd^{3+} (PS, PG and PI) (51, 52), only Gd^{3+} treatment of
253 inside-out patches would be expected to show lipid-mediated inhibition. Indeed, we did not
254 observe consistent Gd^{3+} inhibition in outside-out patches (Fig. 3*C*), and conclude that, like MscL,

255 MSL10 is likely to be inhibited by gadolinium ions indirectly through changes in lipid packing or
256 increased membrane stiffness.
257
258 ***3) Gating dynamics.*** The hallmark of MSL10 activation is a dramatic asymmetry of current
259 (hysteresis) with respect to the pressure ramp, suggesting that the membrane tension at which
260 MSL10 opens is higher than the tension at which it later closes. We reproducibly observed this
261 behavior in experiments with pipettes of various diameters (BN 4 to 7), at opposite membrane
262 potentials, under both positive and negative pipette pressures, with different ramp speeds,
263 buffer compositions and number of channels activated, making it unlikely to be an artifact (Figs.
264 1*,* 4*,* S2, S3). The threshold tension for MSL10 opening depended on ramp speed (in the 1-25s
265 range), decreasing on longer ramps; almost no effect on midpoint tension was seen with MscS
266 opening (33), and no dependence on ramp speed was reported for MSC1 opening (17). Unlike
267 MscS, the unusually slow closing kinetics of both MSL10 and MSC1 were not substantially
268 affected by pressure ramp speed. These observations could be explained by different tension
269 dependencies of opening and closing. The relaxation of the outer leaflet of the membrane in an
270 excised patch described in (53) has little effect on the tension at which MSL10 closes, as it
271 stayed very close to zero in the majority of our experiments regardless of the ramp speed.
272
273 A related feature of MSL10 activity is its behavior in response to application of sharp pressure
274 steps (Fig. 4*C* and S2*B*). Under these conditions, residual MSL10 channel activity in the absence
275 of applied pressure (corresponding to no or very weak membrane tension (54)) was frequently
276 observed after application of the threshold tension, though never before it. Interestingly, MscS
277 demonstrates similar behavior upon closing when the G113A or G121A mutations are
278 introduced (35), indicating that only a small change in identity at a key position (G113 forms a

279 sharp kink in the TM3 of MscS (39)) can produce this phenomenon. Only G121 is conserved in
280 MSC1; neither G113 nor G121 is conserved in MSL10 (Fig. S1*C*). Bulky residues at these
281 positions may make the pore-lining helix of MSL10 stiffer and allow the channel to maintain the
282 open state for a longer period of time, even when little or no membrane tension is applied.
283
284 In summary, MSL10 resembles MSC1 and MscM with respect to unitary channel conductance,
285 MSC1 with respect to ion selectivity, and MSC1 and MscS G113A/MscS 121A with respect to
286 gating kinetics. The similarities and differences between these four channels cannot be easily
287 attributed to sequences previously identified as conserved among MscS family members or
288 important for MscS channel function (summarized in (40)). Instead, these comparisons of
289 sequence and electrophysiological characteristics show that there are still discoveries to be
290 made regarding the relationship between structure and function in the MscS family of MS
291 channels.
292
293 Our characterization of MSL10 channel behavior also provides insight into its possible *in planta*
294 function. Increased tension in the plasma membrane of a plant cell could result from
295 hypoosmotic swelling, invasion of the cell by a pathogen, or bending of a plant organ. As
296 demonstrated for MscS and MscM (12, 38), the immediate consequences of MSL10 opening
297 could include the release of osmolytes, thereby preventing cell lysis under hypoosmotic shock
298 or mechanical strain. However, its preference for anions leads us to speculate that MSL10
299 opening would also result in the depolarization of the cellular membrane via Cl^- efflux. Once
300 open, MSL10 would allow chloride ions to exit the plant cell until membrane tension was
301 completely relieved. A negative feedback mechanism not present in oocyte membranes, such
302 as interaction with signaling molecules, could promote MSL10 channel closing (as proposed for

303 MSC1 (17)). *In planta*, MSL10 gating could lead to the activation of depolarization-activated
304 Shaker-type potassium channels and depolarization-activated Ca^{2+} channels, driving K^{+} efflux
305 from the cell, leading to the loss of water, to intracellular Ca^{2+} signaling, and possibly the
306 propagation of a systemic signal (55, 56). Thus, the electrophysiological characterization of a
307 MscS homolog from a multicellular system opens up the exciting possibility that some members
308 of this family of MS channels may not only release osmolytes from swelling cells and organelles,
309 but also alter cell physiology and potentially participate in intercellular signaling.

310 **METHODS**

311

312 ***Molecular biology.*** To obtain pOO2-MSL10-GFP, the open reading frame of MSL10 was
313 introduced into the pOO2-GFP vector (21) between the XmaI and BamHI cites. Site-directed
314 mutagenesis was used to introduce two stop codons between MSL10 and GFP sequences in
315 pOO2-MSL10-GFP, creating pOO2-MSL10. Capped cRNA was transcribed *in vitro* by SP6
316 polymerase using the mMessenger mMachine kit (Ambion) and stored at -80^{0}C until use.

317

318 ***Oocyte preparation.*** *Xenopus laevis* oocytes (Dumont stage V or VI) were collected and handled
319 as described (21). GFP signal was visible by confocal microscopy within 48 hours of injection,
320 but we observed increased channel activity after longer incubation times, oocytes were
321 patched 1-3 weeks after injection.

322

323 ***Confocal microscopy****.* Two to ten days after injection with pOO2-MSL10-GFP cRNA, de-
324 vitellinized oocytes (57) were placed on cavity slides and covered with thin coverslips. An
325 Olympus Fluoview-1000 confocal with BX-61 microscope and FV10-ASW Olympus application
326 software suite were used for image acquisition.

327

328 ***Electrophysiology.*** The buffers used were: complete ND96 (96 mM NaCl, 2 mM KCl, 2 mM
329 $CaCl_2$, 1 mM $MgCl_2$, 5 mM Hepes, pH 7.38, specific conductivity 13 mS/cm), TEA-Cl (98 mM TEA-
330 Cl, 5 mM Hepes, 2 mM $MgCl_2$, pH 7.38 adjusted with TEA-OH), and 60 mM $MgCl_2$ (with 2 mM
331 Hepes). All traces were obtained from inside-out (excised) patches except for that shown in Fig
332 3*C*, which came from an outside-out excised patch. Experiments in asymmetric buffers,
333 symmetric high salt buffers and gadolinium-containing buffer utilized Rainin Minipulse3

334 peristaltic pumps. In all measurements with asymmetric buffers liquid junction potentials were
335 corrected after the patch was broken. Electrode potential drift was tested before the
336 experiments and was less than 0.1 mV per 10 min. The rest of materials and methods are as in
337 (21).

ACKNOWLEDGMENTS

We thank Dr. Barbara Pickard and three anonymous reviewers for insightful comments on the manuscript. This project was supported in part by American Recovery and Reinvestment Act (ARRA) funds through grant R01GM084211-01 from the National Institutes of Health to Doug Rees, Rob Phillips, and E. S. H.

344 **REFERENCES**

345

346 1. Monshausen GB & Gilroy S (2009) Feeling green: mechanosensing in plants. *Trends Cell*
347 *Biol* 19(5):228-235.

348 2. Arnadottir J & Chalfie M (2010) Eukaryotic mechanosensitive channels. *Annu Rev*
349 *Biophys* 39:111-137.

350 3. Haswell ES (2007) MscS-Like Proteins in Plants. *Mechanosensitive Ion Channels, Part A,*
351 Current Topics in Membranes, ed Hamill OP), Vol 58.

352 4. Zhang W & Fan LM (2009) Actin dynamics regulates voltage-dependent calcium-
353 permeable channels of the Vicia faba guard cell plasma membrane. *J Integr Plant Biol*
354 51(10):912-921.

355 5. Haswell ES, Peyronnet R, Barbier-Brygoo H, Meyerowitz EM, & Frachisse JM (2008) Two
356 MscS homologs provide mechanosensitive channel activities in the Arabidopsis root.
357 *Curr Biol* 18(10):730-734.

358 6. Nakagawa Y, Katagiri T, Shinozaki K, Qi Z, Tatsumi H, Furuichi T, Kishigami A, Sokabe M,
359 Kojima I, Sato S, Kato T, Tabata S, Iida K, Terashima A, Nakano M, Ikeda M, Yamanaka T,
360 & Iida H (2007) Arabidopsis plasma membrane protein crucial for Ca2+ influx and touch
361 sensing in roots. *Proc Natl Acad Sci U S A* 104(9):3639-3644.

362 7. Kurusu T, Nishikawa D, Yamazaki Y, Gotoh M, Nakano M, Hamada H, Yamanaka T, Iida K,
363 Nakagawa Y, Saji H, Shinozaki K, Iida H, & Kuchitsu K (2012) Plasma membrane protein
364 OsMCA1 is involved in regulation of hypo-osmotic shock-induced Ca2+ influx and
365 modulates generation of reactive oxygen species in cultured rice cells. *BMC Plant Biol*
366 12:11.

367 8. Furuichi T, Iida H, Sokabe M, & Tatsumi H (2012) Expression of Arabidopsis MCA1
368 enhanced mechanosensitive channel activity in the Xenopus laevis oocyte plasma
369 membrane. *Plant signaling & behavior* 7(8).
370 9. Pivetti CD, Yen MR, Miller S, Busch W, Tseng YH, Booth IR, & Saier MH, Jr. (2003) Two
371 families of mechanosensitive channel proteins. *Microbiol Mol Biol Rev* 67(1):66-85, table
372 of contents.
373 10. Booth IR, Rasmussen T, Edwards MD, Black S, Rasmussen A, Bartlett W, & Miller S (2011)
374 Sensing bilayer tension: bacterial mechanosensitive channels and their gating
375 mechanisms. *Biochem Soc Trans* 39(3):733-740.
376 11. Kung C, Martinac B, & Sukharev S (2010) Mechanosensitive channels in microbes. *Annu*
377 *Rev Microbiol* 64:313-329.
378 12. Levina N, Totemeyer S, Stokes NR, Louis P, Jones MA, & Booth IR (1999) Protection of
379 Escherichia coli cells against extreme turgor by activation of MscS and MscL
380 mechanosensitive channels: identification of genes required for MscS activity. *EMBO J*
381 18(7):1730-1737.
382 13. Boer M, Anishkin A, & Sukharev S (2011) Adaptive MscS Gating in the Osmotic
383 Permeability Response in E. coli: The Question of Time. *Biochemistry* 50(19):4087-4096.
384 14. Haswell ES & Meyerowitz EM (2006) MscS-like proteins control plastid size and shape in
385 Arabidopsis thaliana. *Curr Biol* 16(1):1-11.
386 15. Wilson ME, Jensen GS, & Haswell ES (2011) Two mechanosensitive channel homologs
387 influence division ring placement in Arabidopsis chloroplasts. *Plant Cell* 23(8):2939-
388 2949.

389 16. Veley KM, Marshburn S, Clure CE, & Haswell ES (2012) Mechanosensitive channels
390 protect plastids from hypoosmotic stress during normal plant growth. *Curr Biol*
391 22(5):408-413.
392 17. Nakayama Y, Fujiu K, Sokabe M, & Yoshimura K (2007) Molecular and
393 electrophysiological characterization of a mechanosensitive channel expressed in the
394 chloroplasts of Chlamydomonas. *Proc Natl Acad Sci U S A* 104(14):5883-5888.
395 18. Haswell ES, Phillips R, & Rees DC (2011) Mechanosensitive channels: what can they do
396 and how do they do it? *Structure* 19(10):1356-1369.
397 19. Miller AJ & Zhou JJ (2000) Xenopus oocytes as an expression system for plant
398 transporters. *Biochim Biophys Acta* 1465(1-2):343-358.
399 20. Yang XC & Sachs F (1990) Characterization of stretch-activated ion channels in Xenopus
400 oocytes. *J Physiol* 431:103-122.
401 21. Maksaev G & Haswell ES (2011) Expression and characterization of the bacterial
402 mechanosensitive channel MscS in Xenopus laevis oocytes. *J Gen Physiol* 138(6):641-
403 649.
404 22. Lew RR (1996) Pressure regulation of the electrical properties of growing Arabidopsis
405 thaliana L. root hairs. *Plant Physiol* 112(3):1089-1100.
406 23. Bezanilla F & Armstrong CM (1972) Negative conductance caused by entry of sodium
407 and cesium ions into the potassium channels of squid axons. *J Gen Physiol* 60(5):588-
408 608.
409 24. Armstrong CM (1971) Interaction of tetraethylammonium ion derivatives with the
410 potassium channels of giant axons. *J Gen Physiol* 58(4):413-437.
411 25. Stanfield PR (1983) Tetraethylammonium ions and the potassium permeability of
412 excitable cells. *Rev Physiol Biochem Pharmacol* 97:1-67.

413 26. Hille B (1968) Charges and potentials at the nerve surface. Divalent ions and pH. *J Gen*
414 *Physiol* 51(2):221-236.
415 27. Hamill OP & McBride DW, Jr. (1996) The pharmacology of mechanogated membrane ion
416 channels. *Pharmacol Rev* 48(2):231-252.
417 28. Dutta R & Robinson KR (2004) Identification and characterization of stretch-activated
418 ion channels in pollen protoplasts. *Plant Physiol* 135(3):1398-1406.
419 29. Alexandre J & Lassalles JP (1991) Hydrostatic and osmotic pressure activated channel in
420 plant vacuole. *Biophys J* 60(6):1326-1336.
421 30. Ding JP & Pickard BG (1993) Mechanosensory calcium-selective cation channels in
422 epidermal cells. *Plant J* 3(1):83-110.
423 31. Berrier C, Coulombe A, Szabo I, Zoratti M, & Ghazi A (1992) Gadolinium ion inhibits loss
424 of metabolites induced by osmotic shock and large stretch-activated channels in
425 bacteria. *Eur J Biochem* 206(2):559-565.
426 32. Akitake B, Anishkin A, & Sukharev S (2005) The "dashpot" mechanism of stretch-
427 dependent gating in MscS. *J Gen Physiol* 125(2):143-154.
428 33. Belyy V, Kamaraju K, Akitake B, Anishkin A, & Sukharev S (2010) Adaptive behavior of
429 bacterial mechanosensitive channels is coupled to membrane mechanics. *J Gen Physiol*
430 135(6):641-652.
431 34. Priel A, Gil Z, Moy VT, Magleby KL, & Silberberg SD (2007) Ionic requirements for
432 membrane-glass adhesion and giga seal formation in patch-clamp recording. *Biophys J*
433 92(11):3893-3900.
434 35. Akitake B, Anishkin A, Liu N, & Sukharev S (2007) Straightening and sequential buckling
435 of the pore-lining helices define the gating cycle of MscS. *Nat Struct Mol Biol*
436 14(12):1141-1149.

437 36. Spalding EP & Goldsmith M (1993) Activation of K+ Channels in the Plasma Membrane
438 of Arabidopsis by ATP Produced Photosynthetically. *Plant Cell* 5(4):477-484.
439 37. Berrier C, Besnard M, Ajouz B, Coulombe A, & Ghazi A (1996) Multiple mechanosensitive
440 ion channels from Escherichia coli, activated at different thresholds of applied pressure.
441 *J Membr Biol* 151(2):175-187.
442 38. Schumann U, Edwards MD, Rasmussen T, Bartlett W, van West P, & Booth IR (2010)
443 YbdG in Escherichia coli is a threshold-setting mechanosensitive channel with MscM
444 activity. *Proc Natl Acad Sci U S A* 107(28):12664-12669.
445 39. Bass RB, Strop P, Barclay M, & Rees DC (2002) Crystal structure of Escherichia coli MscS,
446 a voltage-modulated and mechanosensitive channel. *Science* 298(5598):1582-1587.
447 40. Balleza D & Gomez-Lagunas F (2009) Conserved motifs in mechanosensitive channels
448 MscL and MscS. *Eur Biophys J* 38(7):1013-1027.
449 41. Edwards MD, Li Y, Kim S, Miller S, Bartlett W, Black S, Dennison S, Iscla I, Blount P, Bowie
450 JU, & Booth IR (2005) Pivotal role of the glycine-rich TM3 helix in gating the MscS
451 mechanosensitive channel. *Nat Struct Mol Biol* 12(2):113-119.
452 42. Miller S, Bartlett W, Chandrasekaran S, Simpson S, Edwards M, & Booth IR (2003)
453 Domain organization of the MscS mechanosensitive channel of Escherichia coli. *EMBO J*
454 22(1):36-46.
455 43. Vasquez V, Sotomayor M, Cordero-Morales J, Schulten K, & Perozo E (2008) A structural
456 mechanism for MscS gating in lipid bilayers. *Science* 321(5893):1210-1214.
457 44. Anishkin A & Sukharev S (2004) Water dynamics and dewetting transitions in the small
458 mechanosensitive channel MscS. *Biophys J* 86(5):2883-2895.
459 45. Sotomayor M, Vasquez V, Perozo E, & Schulten K (2007) Ion conduction through MscS as
460 determined by electrophysiology and simulation. *Biophys J* 92(3):886-902.

461 46. Sukharev S (2002) Purification of the small mechanosensitive channel of Escherichia coli
462 (MscS): the subunit structure, conduction, and gating characteristics in liposomes.
463 *Biophys J* 83(1):290-298.
464 47. Edwards MD, Bartlett W, & Booth IR (2008) Pore mutations of the Escherichia coli MscS
465 channel affect desensitization but not ionic preference. *Biophys J* 94(8):3003-3013.
466 48. Li Y, Moe PC, Chandrasekaran S, Booth IR, & Blount P (2002) Ionic regulation of MscK, a
467 mechanosensitive channel from Escherichia coli. *EMBO J* 21(20):5323-5330.
468 49. Borngen K, Battle AR, Moker N, Morbach S, Marin K, Martinac B, & Kramer R (2010) The
469 properties and contribution of the *Corynebacterium glutamicum* MscS variant to fine-
470 tuning of osmotic adaptation. *Biochim. Biophys. Acta* 1798(11):2141-2149.
471 50. Yang XC & Sachs F (1989) Block of stretch-activated ion channels in Xenopus oocytes by
472 gadolinium and calcium ions. *Science* 243(4894 Pt 1):1068-1071.
473 51. Ermakov YA, Kamaraju K, Sengupta K, & Sukharev S (2010) Gadolinium ions block
474 mechanosensitive channels by altering the packing and lateral pressure of anionic lipids.
475 *Biophys J* 98(6):1018-1027.
476 52. Petcoff DW, Holland WL, & Stith BJ (2008) Lipid levels in sperm, eggs, and during
477 fertilization in Xenopus laevis. *J Lipid Res* 49(11):2365-2378.
478 53. Belyy V, Anishkin A, Kamaraju K, Liu N, & Sukharev S (2010) The tension-transmitting
479 'clutch' in the mechanosensitive channel MscS. *Nat Struct Mol Biol* 17(4):451-458.
480 54. Suchyna TM, Markin VS, & Sachs F (2009) Biophysics and structure of the patch and the
481 gigaseal. *Biophys J* 97(3):738-747.
482 55. Ward JM, Maser P, & Schroeder JI (2009) Plant ion channels: gene families, physiology,
483 and functional genomics analyses. *Annual review of physiology* 71:59-82.

484 56. Roelfsema MR, Hedrich R, & Geiger D (2012) Anion channels: master switches of stress
485 responses. *Trends Plant Sci* 17(4):221-229.
486 57. Stuhmer W (1992) Electrophysiological recording from Xenopus oocytes. *Methods*
487 *Enzymol* 207:319-339.

488 **FIGURE LEGENDS**

489

490 **Figure 1. MSL10 expressed in *Xenopus laevis* oocytes produces a channel activity upon**
491 **membrane stretch.** (A) Confocal image of a portion of an oocyte 5 days after injection with
492 MSL10-GFP cRNA. GFP signal is pseudo-colored green. (B) A representative trace illustrating the
493 activation of MSL10 channels at both negative and positive membrane potentials in the same
494 patch. Pipette bubble number (BN) 6, -70 mmHg. (C) Single channel opening events induced by
495 negative pipette pressure. Membrane potential -50 mV, pipette BN 4. (D) Single channel
496 opening events induced by positive pipette pressure. Membrane potential -40 mV, pipette BN
497 5. Symmetric ND96 buffer was used in B-D.

498

499 **Figure 2. MSL10 and MSL10-GFP single-channel conductance.** (A) The current-voltage curves
500 for untagged MSL10 (open circle) and MSL10-GFP (filled squares) in symmetric ND96 buffer,
501 and for untagged MSL10 in symmetric 98 mM TEA-Cl (filled triangles) (n = 5 oocytes for each
502 protein). Solid and dashed lines represent linear fits for the channels in ND96 and TEA-Cl
503 buffers respectively. (B) A typical trace illustrating the appearance of conductive substates at
504 more negative membrane potentials, in this case -60 mV. Pipette BN 5, symmetric ND96 buffer.

505

506 **Figure 3. Ion selectivity and Gd^{3+} inhibition of MSL10.** (A) Current-voltage curves for MSL10 in
507 symmetric ND96 (96mM NaCl, filled squares) and in asymmetric 100 mM/300 mM NaCl buffer
508 (open circles). E_{Cl-}, reversal potential for Cl^- ions. (B) Single channel conductance under
509 increasing [NaCl] at negative (filled squares) and positive (open circles) membrane potentials.
510 Buffers containing 4 mM $MgCl_2$ and 5 mM Hepes supplemented with 100, 300 or 500mM NaCl
511 were used, membrane potential -30 mV). (C) Representative traces showing MSL10 channel

512 activity in the same outside-out patch (pipette BN 5, membrane potential 40mV) before and
513 after bath perfusion with 100 µM $GdCl_3$. (D-F) Representative traces showing MSL10 channel
514 activity in the same patch before and after perfusion with (D) 100 µM $GdCl_3$, (E) 50 µM $GdCl_3$, or
515 (F) 20 µM $GdCl_3$. In D a trace from the same patch after wash-out is shown at right. Membrane
516 potential -40 mV, BN 5, in symmetric ND96 supplemented with the indicated amounts of $GdCl_3$
517 from the bath side. Pressure applied to the pipette was -60 mmHg in all cases except for the
518 third trace in (D), where the pressure was -90 mmHg.
519
520 **Figure 4. Gating kinetics and inactivation of MSL10.** (A, B) Asymmetric opening and closing
521 kinetics under slow ramp speeds in patches with many (A) and few (B) channels. Dashed lines in
522 (A) indicate the first channel opening and last channel closing events. Both traces are 50
523 seconds long, membrane potential -20 mV, pipette BN 4.5, symmetric ND96 buffer. (C) Slow
524 gating and absence of inactivation under sustained tension. The length of the whole trace is 45
525 seconds. Pipette BN 5, symmetric ND96 buffer, and membrane potential -40 mV.

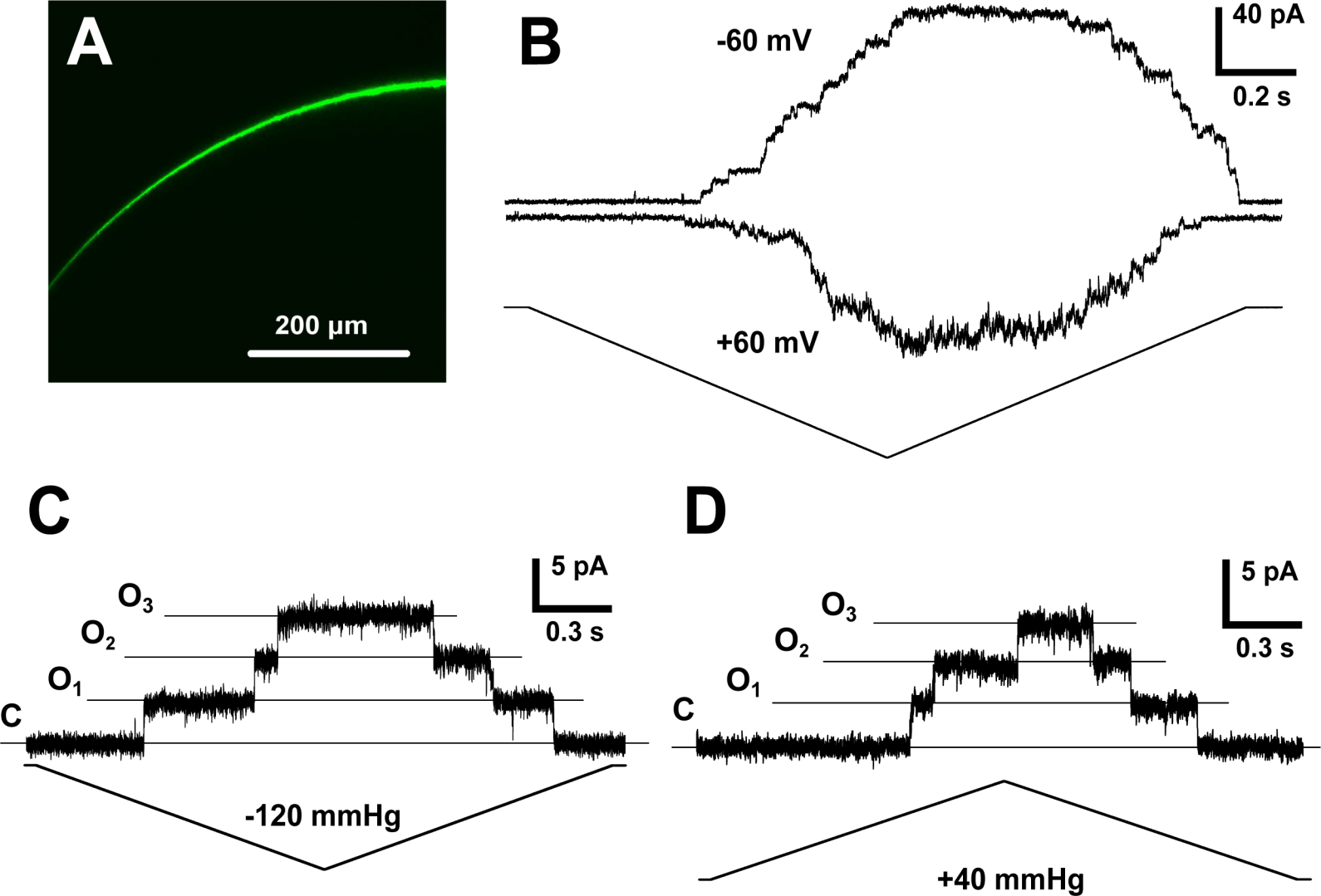
A
200 µm
B
-60 mV
+60 mV
40 pA
0.2 s
C
O3
O2
O1
C
5 pA
0.3 s
-120 mmHg
D
O3
O2
O1
C
5 pA
0.3 s
+40 mmHg

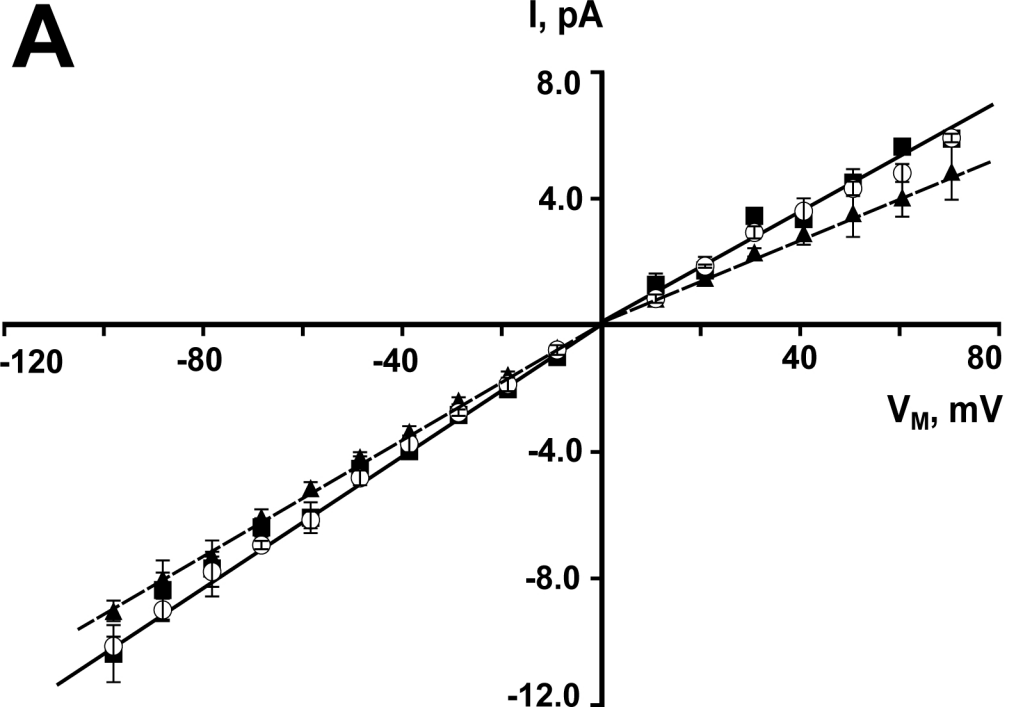
A
I, pA
8.0
4.0
-4.0
-8.0
-12.0
-120
-80
-40
40
80
V_M, mV

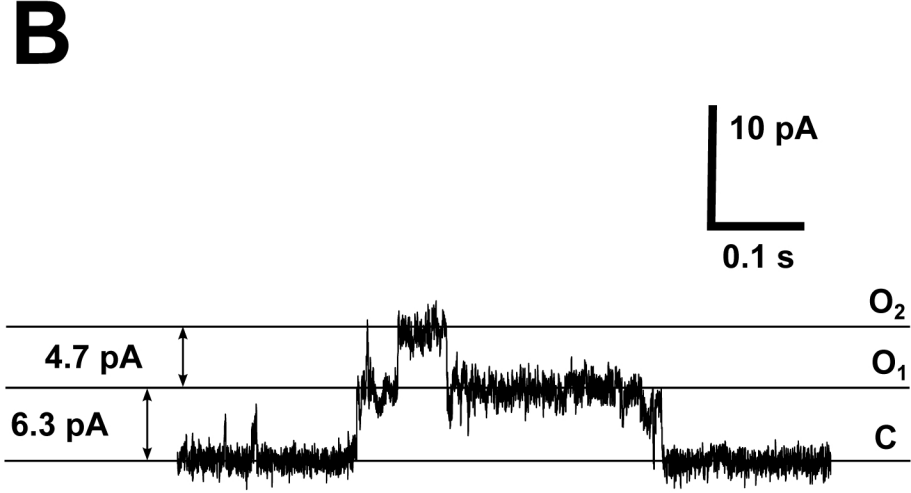
B
10 pA
0.1 s
O_2
O_1
C
4.7 pA
6.3 pA

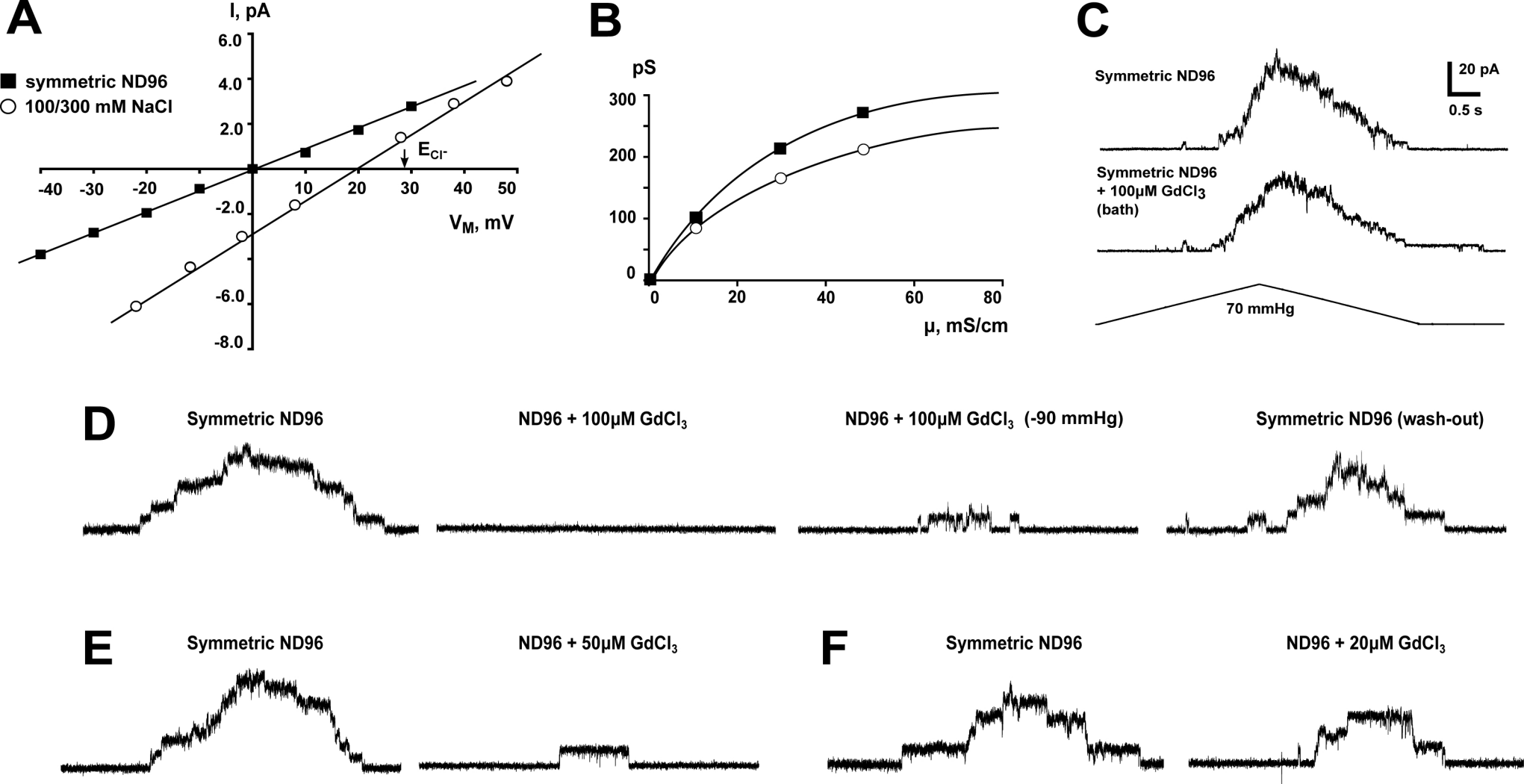
A
I, pA
6.0
4.0
2.0
-2.0
-6.0
-8.0
symmetric ND96
100/300 mM NaCl
E_{Cl^-}
-40 -30 -20 10 20 30 40 50
V_M, mV
B
pS
300
200
100
0
0 20 40 60 80
μ, mS/cm
C
Symmetric ND96
20 pA
0.5 s
Symmetric ND96
+ 100μM $GdCl_3$
(bath)
70 mmHg
D
Symmetric ND96
ND96 + 100μM $GdCl_3$
ND96 + 100μM $GdCl_3$ (-90 mmHg)
Symmetric ND96 (wash-out)
E
Symmetric ND96
ND96 + 50μM $GdCl_3$
F
Symmetric ND96
ND96 + 20μM $GdCl_3$

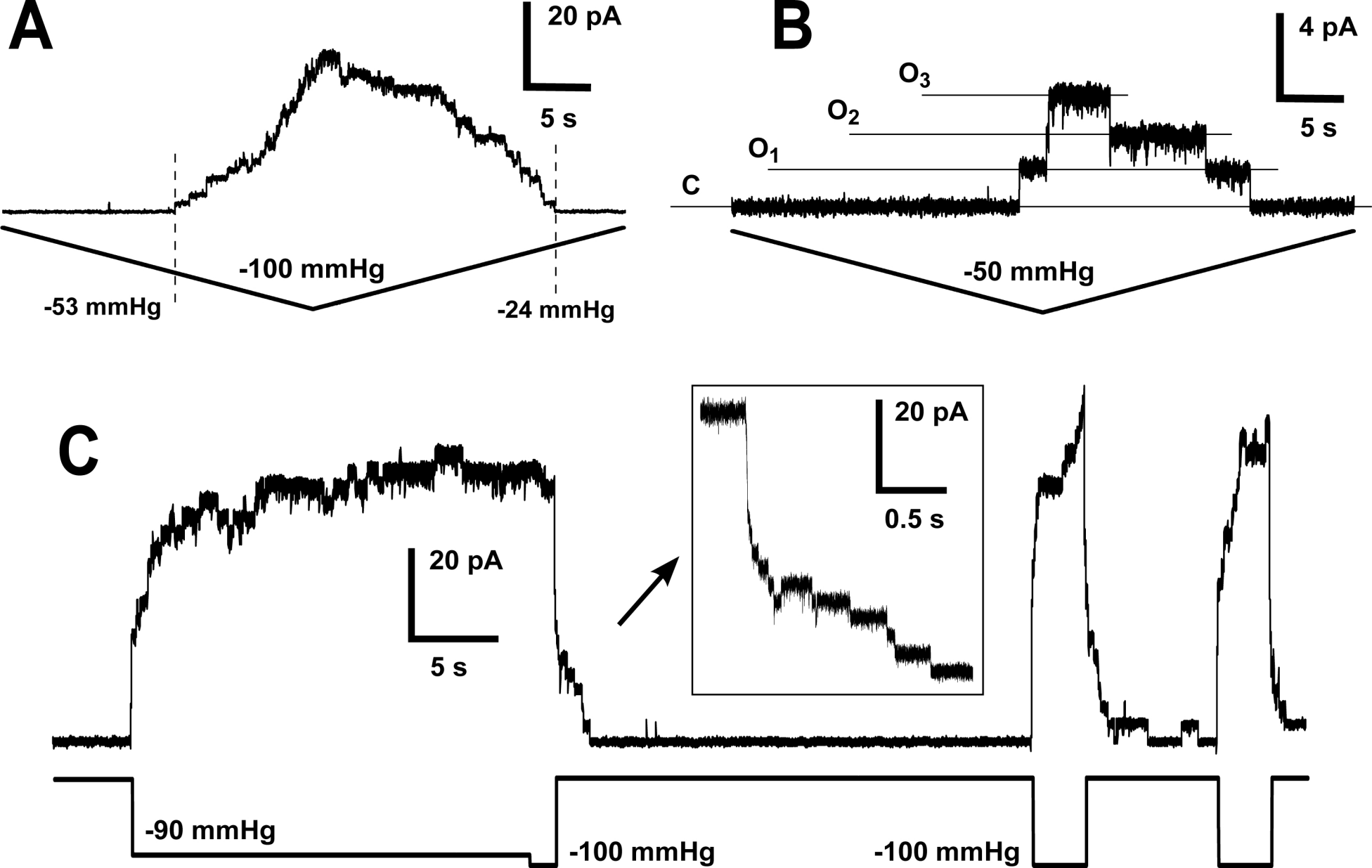
A
20 pA
5 s
-100 mmHg
-53 mmHg
-24 mmHg
B
4 pA
5 s
O3
O2
O1
C
-50 mmHg
C
20 pA
5 s
20 pA
0.5 s
-90 mmHg
-100 mmHg
-100 mmHg

SUPPLEMENTARY FIGURE LEGENDS

Figure S1. Topology and conserved domains of select MscS homologs from bacteria, algae, and plants. (A) Topology of MscS (1) and predicted topology of MscS, MSC1 and MSL10. Dark grey box, chloroplast transit peptide; light grey boxes, transmembrane helices. (B) Ribbon diagram of a single subunit of MscS from the revised crystal structure (PDB 20AU (2, 3)). The conserved MscS domain is indicated in red. (C) Alignment of "MscS domain" sequences from MscS and MscM (*Escherichia coli),* MSC1 (*Chlamydomonas reinhardtii),* and MSL10 (*Arabidopsis thaliana)*. Asterisks indicate conserved residues, **+** signs indicate residues in MscS that produce slow closure when mutated to alanine (4) and dots indicate the two hydrophobic seal residues. Sequences corresponding to TM3a, TM3b, and the β-domain of MscS are as in (2).

Figure S2. MSL10 hysteresis and residual activity in high $MgCl_2$. (A) An example of slow closure of MSL10. Membrane potential -40 mV, BN 5. (B) Residual activity of MSL10 at zero applied tension. Membrane potential -60 mV, BN 4.5. Both A and B were performed in symmetric 60 mM $MgCl_2$ buffer.

Figure S3. Effect of ramp speed on the threshold pressure for MSL10 opening and closing. Traces, obtained from the same patch subject to pressure ramps of various length: 1s (A), 5s (B) and 25s (C). Arrows indicate opening and closing pressure thresholds. Membrane potential -30 mV, pipette BN 5, symmetric ND96 buffer.

Figure S4. Lack of current saturation in MSL10 excised patches. (A) A set of MSL10 dose-response traces from an excised inside-out patch. Arrow indicates the point where the patch

collapsed. (B) Illustration of the easily achievable current saturation and lack of hysteresis in MscS expressed in *Xenopus* oocytes. Dotted lines indicate opening and closing pressure thresholds and dashed lines indicate midpoints of the activation curve. Both traces were recorded from excised inside-out patches from the same batch of oocytes, in symmetric ND96 buffer, pipette BN 4.5, at a membrane potential of -20 mV.

1. Miller S, Bartlett W, Chandrasekaran S, Simpson S, Edwards M, & Booth IR (2003) Domain organization of the MscS mechanosensitive channel of Escherichia coli. *EMBO J* 22(1):36-46.
2. Bass RB, Strop P, Barclay M, & Rees DC (2002) Crystal structure of Escherichia coli MscS, a voltage-modulated and mechanosensitive channel. *Science* 298(5598):1582-1587.
3. Steinbacher S, Bass RB, Strop P, & Rees DC (2007) Structures of the Prokaryotic Mechanosensitive Channels MscL and MscS. *Mechanosensitive Ion Channels, Part A,* Current Topics in Membranes, ed Hamill OP), Vol 58.
4. Akitake B, Anishkin A, Liu N, & Sukharev S (2007) Straightening and sequential buckling of the pore-lining helices define the gating cycle of MscS. *Nat Struct Mol Biol* 14(12):1141-1149.

A

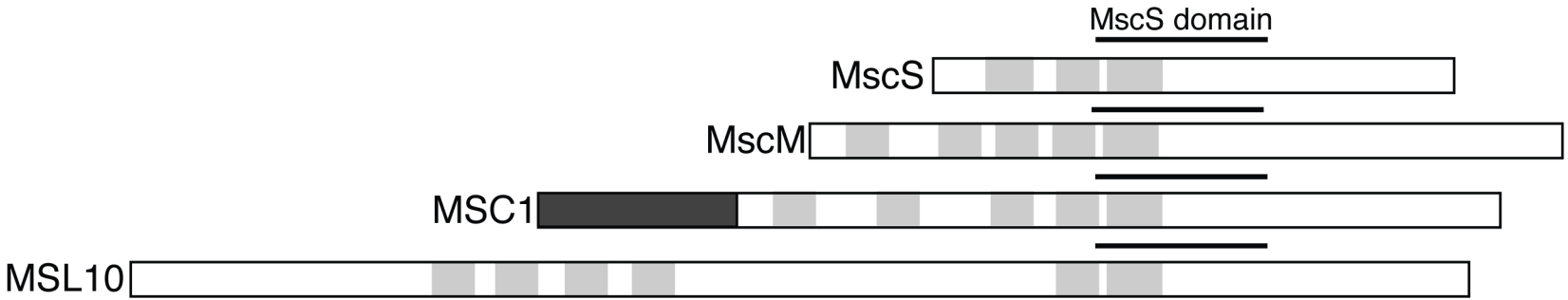
MscS domain
MscS
MscM
MSC1
MSL10

B

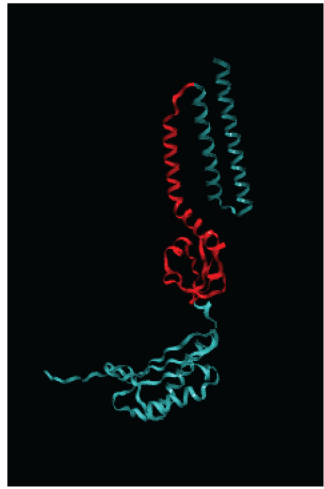

C

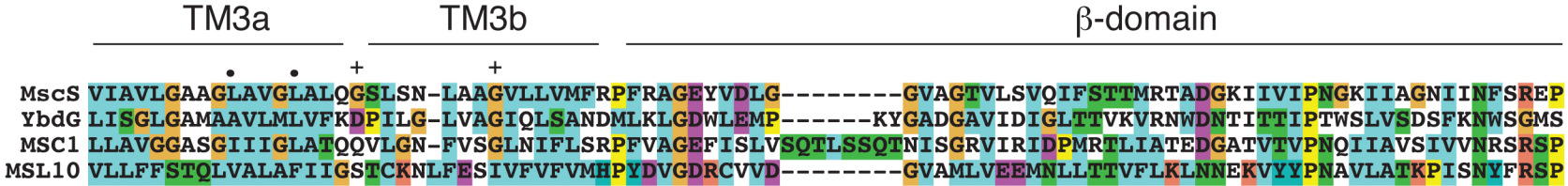
TM3a
TM3b
β-domain
MscS VIAVLGAAGLAVGLALQGSLSN-LAAGVLLVMFRPFRAGEYVDLG--------GVAGTVLSVQIFSTTMRTADGKIIVIPNGKIIAGNIINFSREP
YbdG LISGLGAMAAVLMLVFKDPILG-LVAGIQLSANDMLKLGDWLEMP------KYGADGAVIDIGLTTVKVRNWDNTITTIPTWSLVSDSFKNWSGMS
MSC1 LLAVGGASGIIIGLATQQVLGN-FVSGLNIFLSRPFVAGEFISLVSQTLSSQTNISGRVIRIDPMRTLIATEDGATVTVPNQIIAVSIVVNRSRSP
MSL10 VLLFFSTQLVALAFIIGSTCKNLFESIVFVFVMHPYDVGDRCVVD--------GVAMLVEEMNLLTTVFLKLNNEKVYYPNAVLATKPISNYFRSP

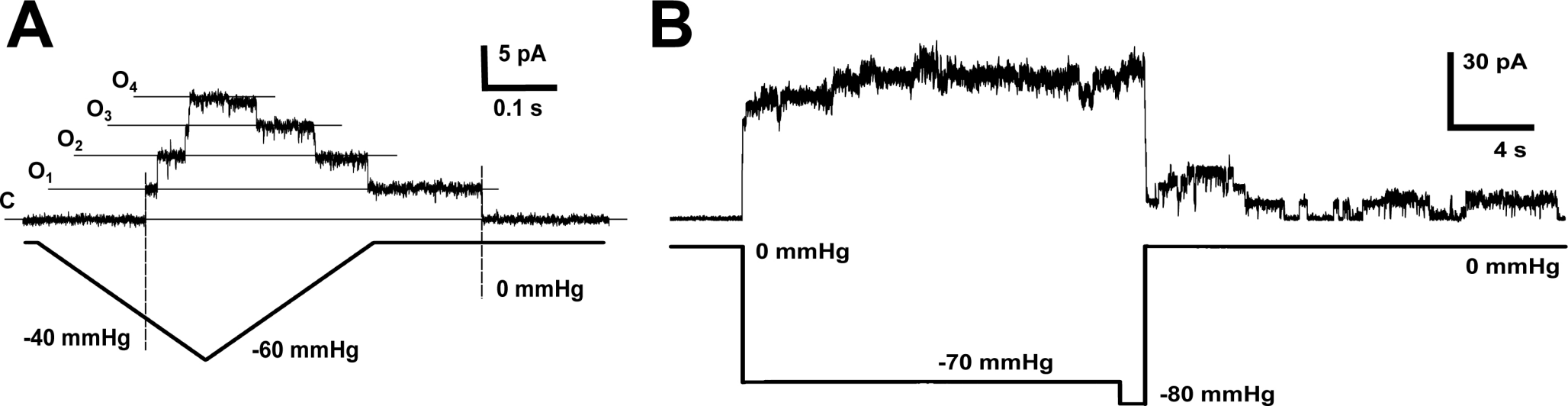
A
5 pA
0.1 s
O4
O3
O2
O1
C
0 mmHg
-40 mmHg
-60 mmHg
B
30 pA
4 s
0 mmHg
0 mmHg
-70 mmHg
-80 mmHg

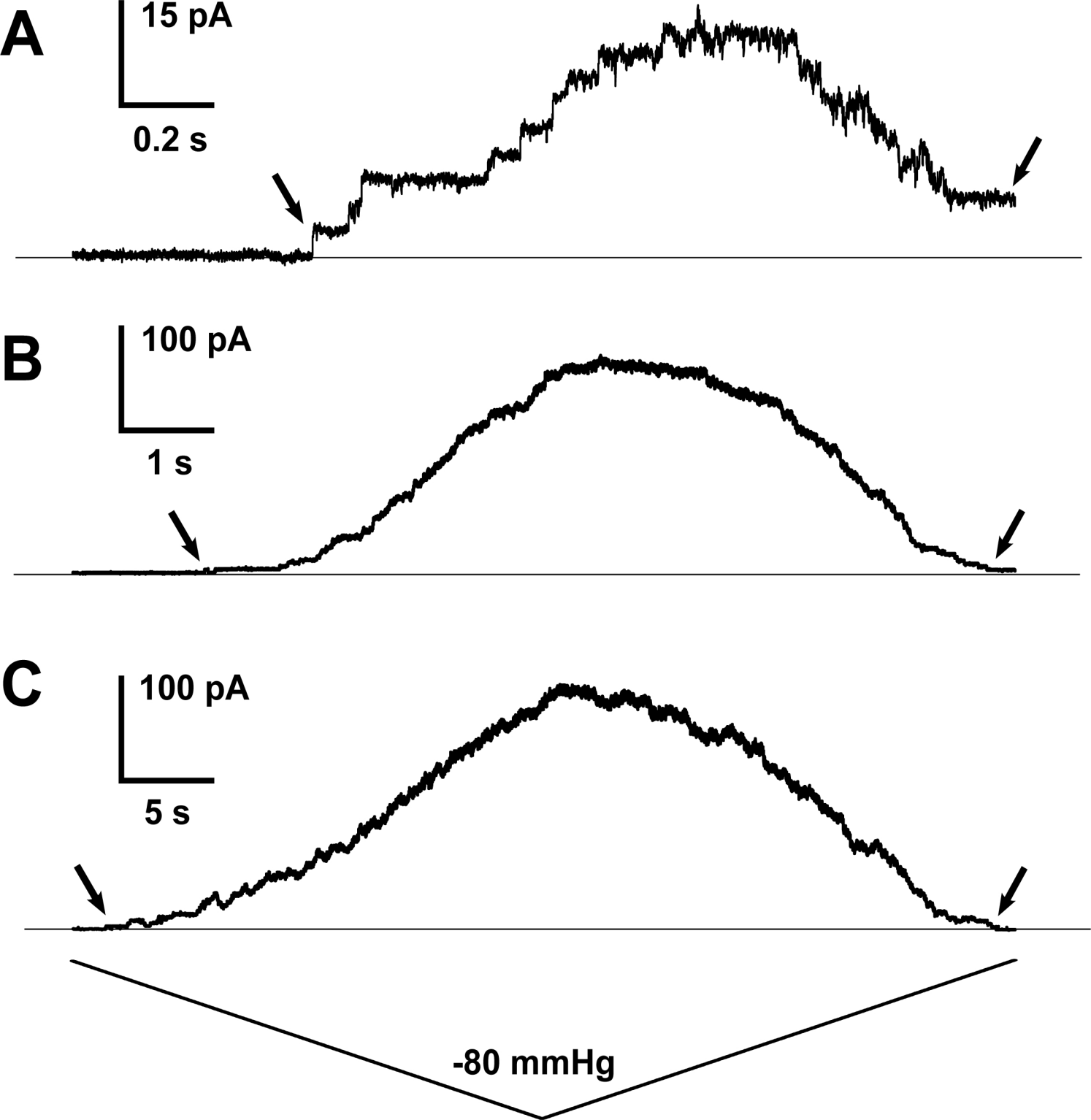
A
15 pA
0.2 s
B
100 pA
1 s
C
100 pA
5 s
-80 mmHg

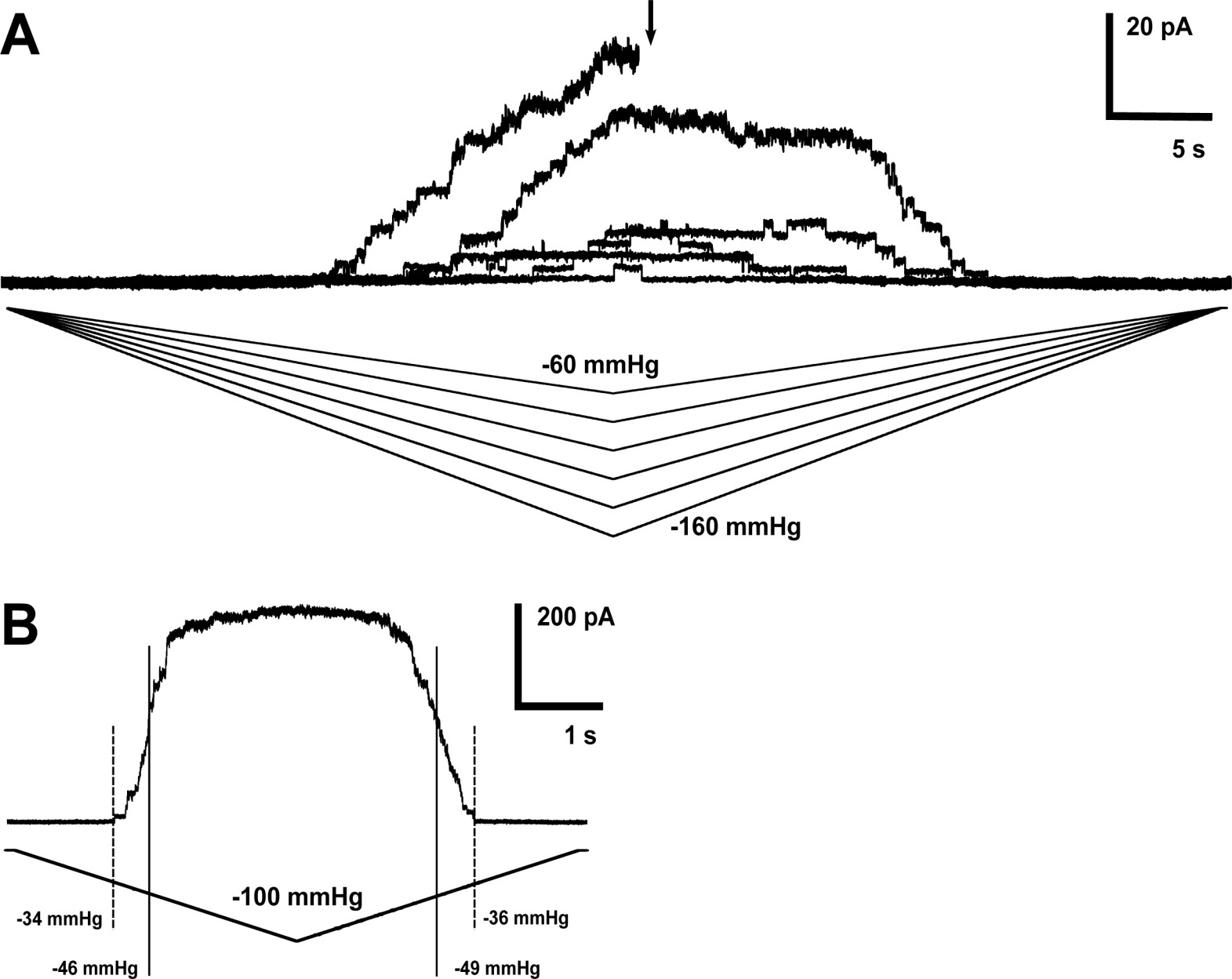
A
20 pA
5 s
-60 mmHg
-160 mmHg
B
200 pA
1 s
-100 mmHg
-34 mmHg
-36 mmHg
-46 mmHg
-49 mmHg